Published in final edited form as:

Nat Struct Mol Biol. 2010 August ; 17(8): 1004–1010. doi:10.1038/nsmb.1867.

Structural basis of Fic mediated adenylylation

Junyu Xiao[1], **Carolyn A. Worby**[1,2,3], **Seema Mattoo**[4], **Banumathi Sankaran**[5], and **Jack E. Dixon**[1,2,3,4]

[1]Department of Pharmacology, University of California, San Diego, La Jolla, CA 92093, USA

[2]Department of Cellular and Molecular Medicine, University of California, San Diego, La Jolla, CA 92093, USA

[3]Department of Chemistry and Biochemistry, University of California, San Diego, La Jolla, CA 92093, USA

[4]Howard Hughes Medical Institute, University of California, San Diego, La Jolla, CA 92093, USA

[5]Berkeley Center for Structural Biology, Lawrence Berkeley Laboratory, 1 Cyclotron Road, Berkeley, CA 94720, USA

Abstract

The Fic family of adenylyltransferases, defined by a core HPFx(D/E)GN(G/K)R motif, consist of over 2700 proteins found from bacteria to humans. IbpA from the bacterial pathogen *Histophilus somni* contains two Fic domains that adenylylate the switch1 Tyr residue of Rho-family GTPases, allowing the bacteria to subvert host defenses. Here we present the structure of the second Fic domain of IbpA (IbpAFic2) in complex with its substrate, Cdc42. IbpAFic2-bound Cdc42 mimics the GDI-bound state of Rho GTPases, with both its switch1 and switch2 regions gripped by IbpAFic2. Mutations disrupting the IbpAFic2-Cdc42 interface impair adenylylation and cytotoxicity. Importantly, the switch1 Tyr of Cdc42 is adenylylated in the structure, providing the first structural view for this post-translational modification. We also demonstrate that the nucleotide-binding mechanism is conserved among Fic proteins, and propose a catalytic mechanism for this recently discovered family of enzymes.

The Fic (filamentation induced by cyclic AMP) domains are defined by a core HPFx(D/E)GN(G/K)R motif and are conserved from bacteria to humans1. Over 2700 Fic proteins exist in nature, and until recently, their biological activity had remained elusive. Orth and colleagues, as well as our laboratory recently reported that Fic domain proteins from two pathogenic bacteria use ATP to catalyze the addition of adenosine monophosphate (AMP) to

Corresponding Author: Jack E. Dixon (jedixon@mail.uscd.edu).

Author contributions J.X. performed most of the research. S.M. purified VopS protein. B.S. collected diffraction data for IbpAFic2 alone crystals. J.X., C.A.W., S.M., J.E.D. designed the research, analyzed data and wrote the manuscript.

Author Information Reprints and permissions information is available at npg.nature.com/reprintsandpermissions. Correspondence and requests for materials should be addressed to J.E.D. (jedixon@ucsd.edu).

Accession codes. Atomic coordinates and structural factors have been deposited in the Protein Data Bank with accession codes 3N3U and 3N3V, for IbpAFic2 and IbpAFic2^{H3717A}-Cdc42 complex, respectively.

Supplementary Information is available on the Nature Structural & Molecular Biology website.

target host proteins2,3. Specifically, IbpA from *Histophilus somni* causes collapse of the host cell actin cytoskeleton by catalyzing the addition of AMP to the three mammalian Rho-family GTPases, RhoA, Rac1, and Cdc422,4. The modification occurs on a conserved tyrosine residue in the switch1 region of these GTPases, resulting in their inability to interact with the downstream effectors. In contrast, VopS from *Vibrio parahaemolyticus* catalyzes the addition of AMP to a conserved switch1 threonine residue in the same family of GTPases3.

It is highly likely that all Fic proteins use the conserved HPFx(D/E)GN(G/K)R motif to catalyze the addition of AMP, or "adenylylation" of target proteins. A small branch of the Fic proteins, known as Doc (death on curing), has been previously studied in the bacteriophage P1 of *E. coli* as part of a toxin-antitoxin module5. Doc triggers cytotoxicity by associating with the 30s ribosomal subunits and inhibiting translation elongation6. The exact nature of Doc function remains unclear; however, Doc also harbors a central HPFx(D/E)GN(G/K)R motif. Mutating the conserved His or Asp in this motif attenuated the cytotoxicity of Doc, suggesting an enzymatic scheme7.

Fic domain-containing proteins are found in many species of bacterial pathogens. In particular, a list of effector proteins from pathogenic bacteria feature this domain, such as AnkX from *Legionella pneumophila*8, BepA from *Bartonella spp.*9, AvrAC from *Xanthomonas campestris*10, and PfhB2 from *Pasteurella multocida*11. It remains to be determined whether these effectors also target the Rho-family GTPases. Structural analyses further expand the Fic/Doc family to include AvrB, an effector protein of the plant pathogen *Pseudomonas syringae*12-14; even though AvrB lacks the HPFx(D/E)GN(G/K)R motif. It is currently unknown whether AvrB represents a functional member of this family. The large number of Fic domain-containing proteins also makes it unlikely that they all function in a pathogenic setting. The presence of a Fic protein, called HYPE (Huntingtin yeast interacting protein E), in higher eukaryotes including humans suggests that Fic-mediated adenylylation might represent a new signaling paradigm that regulates cellular processes2. As such, a deeper understanding of these Fic adenylyltransferases at a structural and functional level will likely shed light on both their physiology and pathology.

The covalent addition of AMP to other proteins has been previously reported. In the late 1960s, adenylylation on tyrosine residues was reported for bacterial glutamine synthetase15,16. Transient adenylylation of a C-terminal glycine residue, or a catalytic lysine residue, also occurs during the activation of ubiquitin/ubiquitinlike proteins17,18, or during DNA/RNA ligation processes19,20. However, the Fic proteins share no homology with bacterial glutamine synthetase adenylyltransferases, the E1-like enzymes, or the polynucleotide ligases. Although structures of several Fic domain proteins have been determined by structural genomics efforts (PDB ID: 2F6S, 2G03, 3CUC, 3EQX, and 2VZA)14,21, they were achieved before the enzymatic activity of this family of proteins was revealed, and did not provide important insights into the catalytic mechanism of these proteins.

IbpA is a large protein that is composed of 4095 amino acids. It contains an N-terminal secretion signal followed by a filamentous hemagglutinin (FHA) domain, which presumably

contributes to its attachment to the host cell22. In its C-terminal region, it contains two consecutive Fic domains (Fic1 and Fic2), which share more than 70% sequence identity (Supplementary Fig. 1) and appear functionally redundant in disrupting the host cell cytoskeleton2. A YopT cysteine protease homology domain resides at the C-terminal end of IbpA; however, this region is dispensable for cytotoxicity2. To further the understanding of the virulence action of *H. somni*, and to gain fundamental insights into the functional mechanism of the Fic proteins, we have performed structural and functional studies on the Fic domain of IbpA. Here we report the crystal structure of IbpAFic2 in complex with Cdc42. Importantly, our structure captures an end product of the enzymatic reaction, in which the switch1 Tyr of Cdc42 is adenylylated. Further, we have elucidated the nucleotide-binding mechanism of IbpAFic2, which is conserved and can be extrapolated to other Fic proteins. Together, these results significantly expand our understanding of this unique family of enzymes and provide compelling new insights into the functional mechanism of these proteins.

RESULTS

Structure of IbpAFic2

IbpAFic2, composed of amino acids 3482-3797 of IbpA, is highly stable and has a similar catalytic activity to larger fragments of Fic1 or Fic2. It crystallized under a condition containing zinc sulfate; and the presence of zinc in the crystal is detected by fluorescence scanning at the synchrotron, even after the crystal is pre-washed with zinc-free solution. As such, we have been able to determine the structure of IbpAFic2 using the Zn-SAD (single-wavelength anomalous dispersion) method (Table 1). The structure is refined to a final 1.85 Å resolution and reveals two zinc atoms bound per IbpAFic2 molecule, which are critical for mediating the crystal contact.

The overall structure of IbpAFic2 reveals an all-helical molecule, containing 14 α-helices. It consists of two segments: an N-terminal helical module and a core Fic domain (Fig. 1). The core Fic domain has a similar architecture to the Fic domains in other Fic protein structures (Supplementary Fig. 2) including Doc and AvrB, featuring a central helix-turn-helix motif (α11–α12) surrounded by six additional α-helices (α6, α8, α9, α10, α13, and α14). The highly conserved HPFx(D/E)GN(G/K)R sequence motif constitutes the α11–α12 loop as well as the first helical turn of α12. The N-terminal helical module is unique to IbpAFic2. In particular, helices α2, α3, and α4 form an independent “arm” subdomain, which specifically recognizes the Rho-family GTPases (see below). It is intriguing that several of other Fic proteins have also evolved unique structural motifs besides the Fic domains (Supplementary Fig. 2). Based on our knowledge of the structure and function of IbpAFic2, we speculate the unique structural element in each Fic protein is responsible for substrate recognition, while the Fic domains execute a common catalytic function.

Structure of the IbpAFic2^{H3717A}-Cdc42 complex

To gain insights into the substrate binding mechanism of IbpAFic2, we have determined the crystal structure of a catalytically compromised mutant, IbpAFic2^{H3717A} in complex with Cdc42 at 2.3 Å resolution (Table 1, Fig. 2a). Although IbpAFic2 is a monomer in solution

based on gel filtration analysis, as well as in the crystal form described above, it emerges as a dimer in the IbpAFic2^{H3717A}-Cdc42 complex structure, leading to the formation of a 2:2 (IbpAFic2: Cdc42) tetramer in the asymmetric unit (Fig. 2a). There are no interactions between the two Cdc42 molecules in the tetramer. Comparison between the structures of apo and Cdc42-bound IbpAFic2 showed that their overall similarity is high. The root mean square difference between the two structures based on the Cα chains is 0.8 Å. Most of the structural differences are located in the arm domain and the long α9–α10 loop (Supplementary Fig. 3a). In the dimer structure, the N-terminal half of the α9–α10 loop interacts with the backside of the arm domain to form the dimer interface, resulting in slight overall displacements of both regions (Supplementary Fig. 3b). The C-terminal half of the α9–α10 loop (residues 3668–3672), disordered in the monomeric structure, also adopts a concrete conformation and plays a pivotal role in recognizing the switch1 region of Cdc42 (see below). The dimer interface buries ~923 Å^2, or ~6% solvent accessible surface from each protein and is mediated mostly by polar interactions, many through water molecules. The residues involved in dimer formation are largely conserved between Fic1 and Fic2 (Supplementary Table 1). Since there are two Fic domains in IbpA, we cannot rule out the possibility that the Fic domains form dimers or heterodimers within the cell. The functional significance of this remains to be explored.

IbpAFic2-bound Cdc42 mimics the GDI-bound state

Comparison of IbpAFic2-bound Cdc42 with available Rho-family protein structures reveals intriguing similarity to the Rho proteins in their GDI (GDP dissociation inhibitor)-bound states. When the Cdc42 structure in the IbpAFic2^{H3717A}-Cdc42 complex was used to search for similar structures in the protein database, Rac2 and Cdc42 in their GDI-bound conformation were the best two matches (PDB ID: 1DS623 and 1DOA24, respectively). The root mean square deviations of alpha-carbon atoms between IbpAFic2-bound Cdc42 and the GDI-bound Rac2 and Cdc42 are 0.8 Å and 0.6 Å, respectively. Alignments with other Cdc42 structures in different functional states also reveal the switch1 and switch2 regions adopt conformations most similar to the GDI bound state (Fig. 2b).

IbpAFic2^{H3717A}-Cdc42 interface

IbpAFic2 employs a tripartite mechanism of substrate recognition and mainly engages the switch1 and switch2 regions of Cdc42 (Fig. 3a). The binding interface between IbpAFic2 and Cdc42 buries an average of ~1142 Å^2 solvent accessible surface (1170 Å^2 and 1113 Å^2 for the two complexes in the asymmetric unit, respectively) from each protein, with the switch1 and switch2 interfaces each constituting ~440 Å^2 and ~610 Å^2, respectively. A third binding interface involves the β1–α1 loop of Cdc42 and the α13–α14 loop of IbpAFic2. This interface is small (~90 Å^2) compared to the former two interfaces, so we will focus our discussion on the interactions mediated by the switch1 and switch2 regions of Cdc42.

At the switch1 region where the target tyrosine (Tyr32^C, Cdc42 residues are denoted with superscript “C”) is located, the side chains of Tyr32^C and Pro34^C make hydrophobic interactions with side chains of Leu3668 and Lys3670 from the α9–β10 loop of IbpAFic2 (Fig. 3b). In particular, the side chains of Leu3668 and Lys3670 form a “clamp”, which locks the position of the Tyr32^C side chain in the correct orientation for modification.

Mutating Leu3668 and Lys3670 to alanines substantially reduced the activity of IbpAFic2 towards the Rho-family proteins (Fig. 3c). In addition to the hydrophobic contacts, a salt bridge between $Asp38^{C}$ and Lys3533, and three main chain-main chain hydrogen bonds between $Thr35^{C}$, $Val33^{C}$ and Asn3667, Thr3669 also contribute to the interaction between IbpAFic2 and Cdc42 at this region.

The binding interface at the switch2 region is more extensive than that at the switch1 region and is mediated by the arm domain of IbpAFic2 (Fig. 3d). The side chains of $Tyr64^{C}$, $Arg66^{C}$, $Leu67^{C}$, $Leu70^{C}$, and $Pro73^{C}$ pack against a hydrophobic patch on the surface of the IbpAFic2 arm domain, formed by Ile3535, Pro3536, Thr3539, Met3543, Phe3549, Ile3552, Leu3553, Gly3556, Ala3557, and Val3560. Several polar interactions are also present at this area, including two salt bridges formed between $Asp63^{C}$ and Arg3563, and between $Arg66^{C}$ and Glu3555. To assess the functional importance of the arm domain, two double mutants, I3535E/P3536E and I3552E/L3553E, were generated. Both mutants display impaired activity towards the Rho-family proteins (Fig. 3c). Reciprocally, a triple mutant of Cdc42 at the switch2 region, Y64A/L67E/L70E, is completely inert as substrate of IbpAFic2; and so are equivalent mutants of Rac1 (Y64A/L67E/L70E) and RhoA (Y66A/L69E/L72E) (Fig. 3e). These data indicate the arm domain dictates the ability of IbpAFic2 to recognize the Rho-family proteins *via* their switch2 regions, and are consistent with our observation that the switch1 region peptide is not a good substrate of IbpAFic2 (data not shown). Interestingly, the same Y/L/L residues are also required for VopS-mediated adenylylation (Fig. 3e). Although VopS adenylylates Rac1, RhoA, and Cdc42 at a threonine residue, our data suggest that VopS might recognize the Rho-family proteins in a manner analogous to IbpAFic2. In agreement with our hypothesis, the recent reported structure of VopS shows that it contains a segment that resembles the arm domain of IbpAFic225.

A snapshot of Fic mediated adenylylation

Although $IbpAFic2^{H3717A}$, a catalytically compromised mutant was used in the co-crystallization experiments, the Tyr32 residues of both Cdc42 molecules in the crystal asymmetric unit are adenylylated (Fig. 4a, Supplementary Fig. 4a). We reason this is caused by the residual enzyme activity of the mutant protein (Supplementary Fig. 4b) in conjugation with a long growth time for the crystals (several weeks). The AMP moiety attached to the Cdc42 molecule provides us with the first snapshot of this post-translational modification at the molecule level. Since our complex structure essentially captures an end product of the enzymatic reaction, it also sheds light on the catalytic mechanism of IbpAFic2 and the Fic domain-containing proteins in general.

The AMP moiety is bound within a surface pocket of IbpAFic2. The adenosine group of AMP is partially enclosed in a hydrophobic environment created by IbpAFic2 residues Ala3673, Phe3675, Ile3714, Gly3724, Pro3752, Ile3754, and Ile3755 (Fig. 3a, 4b). This hydrophobic environment is critical for the function of IbpAFic2. Single amino acid substitution mutants such as A3673E, F3675A, G3724E, and I3755E all have reduced or negligible enzymatic activity (Fig. 3c). Besides the hydrophobic contacts, IbpAFic2 also forms a total of 11 hydrogen bond interactions with AMP, mediated by residues including Lys3670, Glu3671, Asn3672, Gly3722, Asn3723, Gly3724, Arg3728 and Gln3757 (Fig.

4b). In particular, Gly3722, Asn3723, and Gly3724 in the HPFx(D/E)GN(G/K)R motif form four hydrogen bonds with the α-phosphate group of AMP, three of which are contributed by the main chain amide nitrogens of these residues. A sulfate ion binds at approximately the same location in our IbpAFic2 structure (Supplementary Fig. 5) and in two other Fic structures (*H. pylori* Fic and *B. henselae* BepA; PDB ID: 2F6S and 2VZA), suggesting the presence of an "anion hole" at this region. This is reminiscent of the glycine-rich phosphate-binding loops (P-loops) commonly seen in other nucleotide-binding proteins26. Two other residues important for hydrogen bonding with AMP are Arg3728 and Gln3757. Arg3728 forms two hydrogen bonds with the ribose group, and thus serves as an important anchor at the middle of the adenine nucleotide. Gln3757 contributes two hydrogen bonds to interact with the adenine ring. Accordingly, R3728A/Q3757A, a double mutant of IbpAFic2 also has reduced enzymatic activity compared with the wild-type protein (Fig. 3c).

The three major elements involved in nucleotide binding: hydrophobic adenosine-binding pocket, ribose-coordinating arginine, and P-loop are generally conserved in all the available Fic structures. When other Fic structures are superimposed on IbpAFic2, hydrophobic side chains are commonly seen in the vicinity of IbpAFic2 residues Ala3673, Phe3675, Ile3714, Pro3752, Ile3754, and Ile3755 (Fig. 4c, 4d, Supplementary Fig. 6). Similarly, a conserved arginine always exists at the position corresponding to Arg3728 in IbpAFic2. α-Phosphate binding is largely mediated by the highly conserved HPFx(D/E)GN(G/K)R motif. These recurrent features again suggest that all the Fic domains perform a similar catalytic function. The substrates for most of the Fic proteins are currently unknown; however, we and other researchers have noticed that these proteins can auto-adenylylate *in vitro* in the presence of ATP14. It is currently unclear whether this auto-adenylylation activity represents a non-specific reaction or has functional consequences. Nevertheless, it provides us with a tool to probe the putative ATP binding site in these proteins. Mutation of residues corresponding to IbpAFic2 amino acids Phe3675, Gly3724, and Arg3728 in two of these proteins, *N. meningitidis* Fic (Fig. 4c) and *H. pylori* Fic (Fig. 4d), substantially reduced their auto-adenylylation (Fig. 4e). These data further support the hypothesis that the ATP-binding mechanism is generally conserved in all the Fic proteins.

IbpAFic2 mutants display reduced cytotoxicity

In mammalian cells, the Fic domains of IbpA mediated adenylylation of the Rho-family proteins causes collapse of the actin cytoskeleton and drastic cell rounding2,27. To further validate the biological importance of our findings from above analyses, we expressed the various IbpAFic2 mutants as GFP fusion proteins in HeLa cells and evaluated their cytotoxicity. Changes in cell morphology were monitored by fluorescence microscopy (Fig. 5a). The nucleotide-binding mutant G3724E, which failed to adenylylate any of the Rho-family proteins *in vitro*, also completely lost its cell-rounding activity *in vivo*, highlighting the importance of this conserved glycine residue. This result was almost identical to that of the catalytically compromised histidine mutant H3717A. In addition, approximately 50% of the cells expressing I3552E/L3553E (switch2-binding) or L3668A/K3670A (switch1-binding), and 20% of the cells expressing R3728A/Q3757A (nucleotid-binding) remained morphologically normal, indicating a partial loss of function of IbpAFic2 due to these particular mutations (Fig. 5b). The severity of cytotoxicity correlated with the protein

expression levels of these mutants as visualized by GFP intensity. Finally, three other mutants retaining reasonably high enzymatic activity (I3535E/P3536E, F3675A, and I3755E, Fig. 3c) were still capable of inducing pronounced cell rounding (data not shown). Overall, our *in vivo* cytotoxicity results mirror the in vitro adenylylation activities of the IbpAFic2 mutants.

A possible catalytic mechanism

His3717 in IbpAFic2 is part of the highly conserved HPFx(D/E)GN(G/K)R motif. Mutation of this residue significantly lowers the adenylyltransferase activity2. There are two possible ways that this histidine could contribute to catalysis. It could be involved in forming a covalent histidine-AMP intermediate, analogous to the phosphoramidate intermediate during DNA/RNA ligase funciton19,20, and then transfer the AMP group to the Rho proteins. The fact that the Fic proteins can auto adenylylate appears to be consistent with this hypothesis. However, several lines of evidence argue against this scenario. First, the H3717A mutant is not completely inactive (Supplementary Fig. 4b). In fact, it catalyzed the adenylylation of Cdc42 in our complex crystal (Fig. 2a). Second, if an enzyme-AMP intermediate is formed during catalysis, one would expect to see the accumulation of this intermediate if the substrate is not adenylylation competent, for example, in the presence of the Y32F mutant of Cdc42. However, this appears to be not the case (Supplementary Fig. 7). Furthermore, our attempts to capture an enzyme-AMP intermediate by soaking IbpAFic2 crystals in ATP-containing solutions were not successful (data not shown). Although we are still not certain about the nature and function of the auto-adenylylation, the structural information we have obtained strongly suggests that the highly conserved histidine in the HPFx(D/E)GN(G/K)R motif functions as a general base during catalysis.

As shown in Fig. 6a, structural superposition of wild-type IbpAFic2 and IbpAFic2^{H3717A} revealed little geometric alteration in the positions of the residues in the active site region. We can thus examine the position of His3717 of the wild-type structure to evaluate its role during catalysis. Assuming the side chain of His3717 adopts the same rotamer orientation as seen in the crystal structure, its NE atom will be only ~2.2 Å away from the O1P atom of the adenylylated tyrosine, which presumably corresponds to the hydroxyl group oxygen of the unmodified tyrosine (Fig. 6a). This strongly suggests that the histidine functions to attract a proton from the tyrosine, which will prepare the tyrosine as a nucleophile to attack the α-phosphate of ATP (Fig. 6b). This substrate-assisted attack of ATP is also consistent with our observation that IbpAFic2 hydrolyzes ATP very slowly in the absence of Rho GTPases (~8 molecules of AMP generated per molecule of IbpAFic2 per hour at 30 °C, Supplementary Fig. 8).

DISCUSSION

In the late 1960s, the Stadtman laboratory reported that *E. coli* glutamine synthetase (GS) is modified on a Tyr residue by the addition of AMP. This modification, named “adenylylation”, plays a key role in regulating GS activity. As such, adenylylation was demonstrated for the first time as a novel type of post-translational modification. However, the concept of protein adenylylation has remained largely quiescent until recently. As

described earlier, both IbpA and VopS can elicit cytotoxicity by adenylylating Rho-family GTPases, albeit targeting different residues. These two proteins share no overall sequence homology, except at a conserved HPFx(D/E)GN(G/K)R motif. This motif is found in ~2700 bacterial proteins and has a single copy in the human genome. The function of the human protein, known as HYPE is currently unclear; however it also has the ability to adenylylate Rho GTPases *in vitro*2. Collectively, these findings suggest that adenylylation is a widely used post-translational modification present in both prokaryotes and eukaryotes.

We have characterized the structure of a ternary complex containing IbpAFic2 and adenylylated Cdc42. Our structure elucidates the nucleotide-binding mechanism of the Fic proteins. Based on our structure-based analysis, we can further predict residues that are important for nucleotide binding in other Fic proteins. For example, we have shown that by mutating relevant residues, we can disrupt the auto-adenylylation of two other Fic proteins: *N. meningitidis* Fic and *H. pylori* Fic (Fig. 4e). The active site architecture also leads us to propose a catalytic mechanism used by IbpAFic2 and possibly all Fic proteins, involving the highly conserved histidine as the general base (Fig. 6b). In IbpAFic2, the side chain orientation of this histidine appears to be stabilized by the ring stacking interaction from residue Phe3675 to further assist catalysis (Fig. 6a). Curiously, a ring-featured side chain appears to be a common feature for residues corresponding to IbpAFic2 Phe3675 in many other Fic structures, and a phenylalanine is highly preferred (Fig. 4c, 4d, Supplementary Fig. 6). We also speculate the P-loop within the HPFx(D/E)GN(G/K)R motif might contribute to stabilize the negatively charged pentahedral intermediate during catalysis. The β and γ phosphates of ATP are most likely complexed with a Mg^{2+} ion to facilitate the formation of pyrophosphate as a leaving group (Fig. 6b). The rest of the HPFx(D/E)GN(G/K)R motif residues such as Pro3718, Phe3719, Ala3720, and Glu3721 in IbpAFic2, potentially make contacts with the Mg^{2+}/β, γ-pyrophosphate, as suggested by their spatial location in reference to the AMP moiety in our complex structure. This will make the β, γ-pyrophosphate a better leaving group to complete the catalytic reaction. Many aspects of our herein proposed catalytic mechanism is supported by a recent kinetic study on VopS25.

We have also unraveled how IbpAFic2 specifically targets the switch1 Tyr residue of Rho-family GTPases. IbpAFic2 recognizes a 3D epitope in the Rho-family proteins, which involves their critical switch1 and switch2 regions, resulting in tight substrate specificity. The interaction is mediated by the arm domain and the Leu3668-Lys3670 clamp of IbpAFic2. Other proteins work on different substrates where alternative amino acid residues could be adenylylated. We have shown that VopS also requires a proper switch2 region in the Rho-family proteins for function. Consistent with our results, the recent published VopS structure reveals an IbpAFic2 arm like segment (PDB ID: 3LET)25. Superposing VopS onto IbpAFic2 in our complex structure suggests that this segment is in a perfect position to interact with the switch2 region of Cdc42 (Supplementary Fig. 9). Nevertheless, VopS must contain distinct structural elements that account for its modification of the threonine instead of the tyrosine residue. Our modeled VopS–Cdc42 structure suggests that the long α2–α3 loop in the C-terminal domain of VopS is most likely responsible for determining this specificity. However, several side-chain clashes exist between this region and the switch2

region of Cdc42 in this model, suggesting this region likely undergoes a conformational change upon substrate binding.

Interestingly, IbpAFic2-bound Cdc42 adopts a GDI-bound conformation in the complex structure. This is reminiscent of the effect that *Yersinia* effector YpkA exerts on the Rho-family proteins28, and might be another example of the molecular mimicry strategy commonly employed by bacterial effectors29,30. Our complex structure suggests that IbpAFic2 has the ability to elicit a conformational change in the Rho-family proteins and convert them into their inactive GDI-bound conformation. The GDI proteins can bind to both the GDP-bound and GTP-bound forms of the small GTPases and inhibit their functions24,31. By exerting a GDI-mimicry activity, IbpA could pursue the Rho-family proteins irrespective of their functional states in the cell. This is borne out by our crystal structure, which suggests GDP-bound Cdc42 can be adenylylated by IbpAFic2 (Fig. 2a).

In summary, we have determined the crystal structures of IbpAFic2, by itself and in complex with its reaction product, adenylylated Cdc42. The structural information, coupled with biochemical and cell biology experiments, has provided fundamental insights to the molecular mechanism of IbpAFic2 function and may facilitate the design of therapeutically important inhibitors. Our study also sheds light on the catalytic process of Fic mediated adenylylation, and we propose that our suggested catalytic mechanism is likely used by many of the more than 2700 Fic proteins.

Supplementary Material

Refer to Web version on PubMed Central for supplementary material.

Acknowledgements

We are grateful to the UCSD X-ray facility staff and the Advanced Light Source (beam line 8.2.1) staff of Lawrence Berkeley National Laboratory for beam access and help with data collection. We thank Drs. Zhaohui Xu and Xing Guo for critically reading the manuscript and members of the Dixon laboratory for helpful discussions. This work was supported by the National Institutes of Health AI060662 to J.E.D.

Appendix

ONLINE METHODS

Protein expression and purification

Plasmids encoding IbpA$^{3482\text{-}3797}$ and Cdc42$^{1\text{-}181}$ were expressed in *E. coli* strain BL21-CodonPlus(DE3)-RIPL (Stratagene). IbpA$^{3482\text{-}3797}$ was expressed using a modified pET28a vector as a His$_6$-SUMO fusion protein. Cdc42$^{1\text{-}181}$ was expressed using a modified pGEX-4T1 vector with a tobacco etch virus (TEV) cleavage site engineered between GST and Cdc42. For protein expression, cultures were grown at 37°C in LB medium to an OD_{600} of 0.8 before induced with 0.4 mM IPTG at room temperature for overnight. Cells were harvested by centrifugation and frozen at −80°C.

His$_6$-SUMO-IbpA$^{3482\text{-}3797}$ was purified by Ni-NTA affinity chromatography and digested with the SUMO specific protease ULP1. His$_6$-SUMO and the ULP1 protease were removed

by a second Ni-NTA affinity chromatography. Untagged IbpA$^{3482-3797}$ was further purified by anion exchange and gel filtration chromatography. Purified protein was concentrated to 25 mg ml^{-1}, flash-frozen with liquid nitrogen, and stored at −80°C. The H3717A mutant was purified similarly.

GST-Cdc42$^{1-181}$ was purified by GST affinity chromatography. After overnight digestion by TEV protease to cleave off the GST tag, untagged Cdc42$^{1-181}$ was further isolated from the digestion mixture and purified by anion exchange chromatography. Purified Cdc42 was concentrated to 6 mg ml^{-1} and flash-frozen with liquid nitrogen. More details of protein purification are presented in **Supplementary Methods.**

Crystallization

IbpAFic2 alone crystals were grown at 4°C via sitting-drop vapor diffusion method, using a 1:1 ratio of protein: reservoir solution containing 24-28% (v/v) PEG MME 550, 100 mM MES (pH 6.5), and 1-1.5 mM $ZnSO_4$. Crystals grew to full size in several days and were transferred to 32.5% (v/v) PEG MME 550, 100 mM MES (pH 6.5), and 1 mM ZnSO4 before flash-frozen under liquid nitrogen. To prepare the zinc derivative for phase determination, crystals obtained above were back soaked twice in 32.5% (v/v) PEG MME 550, and 100 mM MES (pH 6.5) before frozen.

To obtain the IbpAFic2^{H3717A}-Cdc42 complex crystals, purified IbpAFic2^{H3717A} and Cdc42 were mixed at a 1:1 molar ratio, buffer exchanged into 25 mM Tris (pH 7.5), 25 mM NaCl, 2 mM DTT, 2 mM $MgCl_2$, and 2 mM ATP, and concentrated to ~ 25 mg ml^{-1}. The protein mixture was incubated on ice for another 2 hours before subjected to crystal screen. The best crystal was obtained at 4°C from a sitting-drop vapor diffusion sample where the complex was mixed with equal volume of reservoir solution containing 25% (w/v) PEG 3350, 100 mM Bis-Tris (pH 5.5), and 200 mM (NH4)2SO4. Crystals grew to full size in several weeks. For cryo protection, the crystals was transferred to 27% (w/v) PEG 3350, 100 mM Bis-Tris (pH 5.5), 200 mM $(NH_4)_2SO_4$, and 10% (v/v) glycerol before flash-frozen under liquid nitrogen.

Structure determination and analysis

The structure of IbpAFic2 alone was determined by the single-wavelength anomalous dispersion (SAD) method using the data collected from a zinc derivative crystal. The structure of IbpAFic2^{H3717A}-Cdc42 complex was determined by the molecular replacement method. The refined IbpAFic2 structure obtained above and the published Cdc42 structure (PDB ID: 2WM9) were used as search models. More details are presented in **Supplementary Methods.**

Adenylylation Assay

Mutations were introduced into plasmids encoding IbpAFic2, Cdc42$^{1-181}$, Rac1$^{1-184}$, and RhoA$^{1-181}$ by a PCR based method. IbpAFic2 and mutants were expressed as 8xHis fusion protein; and Cdc42, Rac1, RhoA and mutants were expressed as His_6-SUMO fusion proteins. DNA fragments encoding *N. meningitidis* Fic and *H. pylori* Fic were amplified from their each respective genomic DNA (ATCC BAA-335-5 and 700392), and they were

expressed as His_6-SUMO fusion proteins as well. For protein expression, cultures were grown at 37°C in LB medium to an OD_{600} of 0.8 before induced with 0.4 mM IPTG at room temperature for overnight. All proteins used for the adenylylation assay were purified using a Maxwell 16 Instrument (Promega) and the magnetic nickel particles included in the Maxwell 16 Polyhistidine Protein Purification Kit. The lysis buffer and elution buffers are 50 mM Tris (pH 8.0), 300 mM NaCl, 2 mM $MgCl_2$, and 5 mM β-mercaptoethanol; and 50 mM Tris (pH 8.0), 50 mM NaCl, 250 mM imidazole, 2 mM $MgCl_2$, and 5 mM β-mercaptoethanol, respectively. Protein concentration was determined by the Bradford method. Plasmid encoding GST-VopS was kindly provided by Dr. Kim Orth (UT Southwestern), and GST-VopS was purified by standard procedures.

For adenylylation of the Rho-family proteins, approximately 0.3 μg of IbpAFic2 (wild-type or various mutants) or VopS was mixed with 2 μg of His-SUMO-Cdc42/ Rac1/RhoA (wild-type or mutants) in a 40 μl reaction containing 25 mM Tris (pH 7.5), 3 mM $MgCl_2$, 1 mM DTT, 0.5 mM EDTA, 50 μM cold ATP, and 5 μCi α-^{32}PATP. For auto-adenylylation of *N. meningitidis* Fic, *H. pylori* Fic and their mutants, 2 μg of proteins were incubated in the above buffer conditions in the presence of 10 μCi α-^{32}P-ATP. The reactions were incubated at 30°C for 30 min before terminated by adding LDS sample buffer and boiling. Reaction products were separated on SDS gels and visualized by Coomassie staining and autoradiography.

Cell culture, transfection and microscopy

For transfection, DNA fragments encoding IbpAFic2 and mutants were cloned into the pEGFP-C1 vector (Clontech). HeLa cells grown in 6-well plates in DMEM supplemented with 10% (w/v) FBS (fetal bovine serum), 100 units ml^{-1} penicillin and 100 μg ml^{-1} streptomycin were transfected with 2 μg DNA and 6 μl FuGENE6 reagents (Roche). After ~16 hours transfection, the cells were fixed using PBS buffer supplemented with 4% (v/v) paraformaldehyde and 4% (w/v) sucrose for 15 min, and then solubilized using PBS buffer supplemented with 0.1% (v/v) triton X-100 and 3% (w/v) BSA (bovine serum albumin) for 5min. After extensive washes, actin stress fibers were stained with rhodamine phalloidin (1: 500 in PBS supplemented with 3% BSA); and the cells were visualized by fluorescence microscopy.

References

1. InterPro: IPR003812 Filamentation induced by cAMP/death on curing, related. 2010http://www.ebi.ac.uk/interpro/IEntry?ac=IPR003812
2. Worby CA, et al. The fic domain: regulation of cell signaling by adenylylation. Mol Cell. 2009; 34:93–103. [PubMed: 19362538]
3. Yarbrough ML, et al. AMPylation of Rho GTPases by Vibrio VopS disrupts effector binding and downstream signaling. Science. 2009; 323:269–72. [PubMed: 19039103]
4. Zekarias B, et al. Histophilus somni IbpA DR2/Fic in virulence and immunoprotection at the natural host alveolar epithelial barrier. Infect Immun. 2010; 78:1850–8. [PubMed: 20176790]
5. Lehnherr H, Maguin E, Jafri S, Yarmolinsky MB. Plasmid addiction genes of bacteriophage P1: doc, which causes cell death on curing of prophage, and phd, which prevents host death when prophage is retained. J Mol Biol. 1993; 233:414–28. [PubMed: 8411153]

6. Liu M, Zhang Y, Inouye M, Woychik NA. Bacterial addiction module toxin Doc inhibits translation elongation through its association with the 30S ribosomal subunit. Proc Natl Acad Sci U S A. 2008; 105:5885–90. [PubMed: 18398006]
7. Magnuson R, Yarmolinsky MB. Corepression of the P1 addiction operon by Phd and Doc. J Bacteriol. 1998; 180:6342–51. [PubMed: 9829946]
8. Roy CR, Mukherjee S. Bacterial FIC Proteins AMP Up Infection. Sci Signal. 2009; 2:pe14. [PubMed: 19293428]
9. Schmid MC, et al. A translocated bacterial protein protects vascular endothelial cells from apoptosis. PLoS Pathog. 2006; 2:e115. [PubMed: 17121462]
10. Xu RQ, et al. AvrAC(Xcc8004), a type III effector with a leucine-rich repeat domain from Xanthomonas campestris pathovar campestris confers avirulence in vascular tissues of Arabidopsis thaliana ecotype Col-0. J Bacteriol. 2008; 190:343–55. [PubMed: 17951377]
11. May BJ, et al. Complete genomic sequence of Pasteurella multocida, Pm70. Proc Natl Acad Sci U S A. 2001; 98:3460–5. [PubMed: 11248100]
12. Lee CC, et al. Crystal structure of the type III effector AvrB from Pseudomonas syringae. Structure. 2004; 12:487–94. [PubMed: 15016364]
13. Desveaux D, et al. Type III effector activation via nucleotide binding, phosphorylation, and host target interaction. PLoS Pathog. 2007; 3:e48. [PubMed: 17397263]
14. Kinch LN, Yarbrough ML, Orth K, Grishin NV. Fido, a novel AMPylation domain common to fic, doc, and AvrB. PLoS One. 2009; 4:e5818. [PubMed: 19503829]
15. Stadtman ER, Shapiro BM, Kingdon HS, Woolfolk CA, Hubbard JS. Cellular regulation of glutamine synthetase activity in Escherichia coli. Adv Enzyme Regul. 1968; 6:257–89. [PubMed: 4889221]
16. Brown MS, Segal A, Stadtman ER. Modulation of glutamine synthetase adenylylation and deadenylylation is mediated by metabolic transformation of the P II -regulatory protein. Proc Natl Acad Sci U S A. 1971; 68:2949–53. [PubMed: 4399832]
17. Hochstrasser M. Origin and function of ubiquitin-like proteins. Nature. 2009; 458:422–9. [PubMed: 19325621]
18. Kerscher O, Felberbaum R, Hochstrasser M. Modification of proteins by ubiquitin and ubiquitin-like proteins. Annu Rev Cell Dev Biol. 2006; 22:159–80. [PubMed: 16753028]
19. Shuman S, Lima CD. The polynucleotide ligase and RNA capping enzyme superfamily of covalent nucleotidyltransferases. Curr Opin Struct Biol. 2004; 14:757–64. [PubMed: 15582400]
20. Shuman S. DNA ligases: progress and prospects. J Biol Chem. 2009; 284:17365–9. [PubMed: 19329793]
21. Das D, et al. Crystal structure of the Fic (Filamentation induced by cAMP) family protein SO4266 (gi|24375750) from Shewanella oneidensis MR-1 at 1.6 A resolution. Proteins. 2009; 75:264–71. [PubMed: 19127588]
22. Tagawa Y, et al. Genetic and functional analysis of Haemophilus somnus high molecular weight-immunoglobulin binding proteins. Microb Pathog. 2005; 39:159–70. [PubMed: 16169703]
23. Scheffzek K, Stephan I, Jensen ON, Illenberger D, Gierschik P. The Rac-RhoGDI complex and the structural basis for the regulation of Rho proteins by RhoGDI. Nat Struct Biol. 2000; 7:122–6. [PubMed: 10655614]
24. Hoffman GR, Nassar N, Cerione RA. Structure of the Rho family GTPbinding protein Cdc42 in complex with the multifunctional regulator RhoGDI. Cell. 2000; 100:345–56. [PubMed: 10676816]
25. Luong P, et al. Kinetic and structural insights into the mechanism of AMPylation by VopS FIC domain. J Biol Chem. 2010
26. Hirsch AK, Fischer FR, Diederich F. Phosphate recognition in structural biology. Angew Chem Int Ed Engl. 2007; 46:338–52. [PubMed: 17154432]
27. Hoshinoo K, Sasaki K, Tanaka A, Corbeil LB, Tagawa Y. Virulence attributes of Histophilus somni with a deletion mutation in the ibpA gene. Microb Pathog. 2009; 46:273–82. [PubMed: 19269314]

28. Prehna G, Ivanov MI, Bliska JB, Stebbins CE. Yersinia virulence depends on mimicry of host Rho-family nucleotide dissociation inhibitors. Cell. 2006; 126:869–80. [PubMed: 16959567]
29. Galan JE. Common themes in the design and function of bacterial effectors. Cell Host Microbe. 2009; 5:571–9. [PubMed: 19527884]
30. Elde NC, Malik HS. The evolutionary conundrum of pathogen mimicry. Nat Rev Microbiol. 2009; 7:787–97. [PubMed: 19806153]
31. DerMardirossian C, Bokoch GM. GDIs: central regulatory molecules in Rho GTPase activation. Trends Cell Biol. 2005; 15:356–63. [PubMed: 15921909]
32. Rossman KL, et al. A crystallographic view of interactions between Dbs and Cdc42: PH domain-assisted guanine nucleotide exchange. EMBO J. 2002; 21:1315–26. [PubMed: 11889037]
33. Lammers M, Meyer S, Kuhlmann D, Wittinghofer A. Specificity of interactions between mDia isoforms and Rho proteins. J Biol Chem. 2008; 283:35236–46. [PubMed: 18829452]

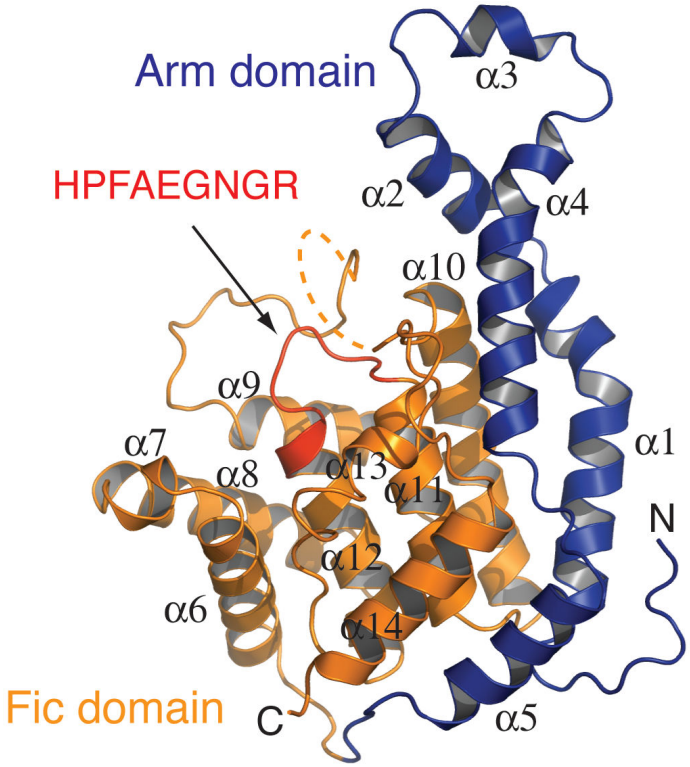

Figure 1.

Ribbon representation of IbpAFic2 structure.

The N-terminal helical motif including the arm domain is colored in blue. The Fic domain is colored in orange. The HPFAEGNGR motif is highlighted in red. Secondary structural elements and the N- and C-termini of the structure are labeled. Part of the α9–α10 loop is disordered and shown as dash lines.

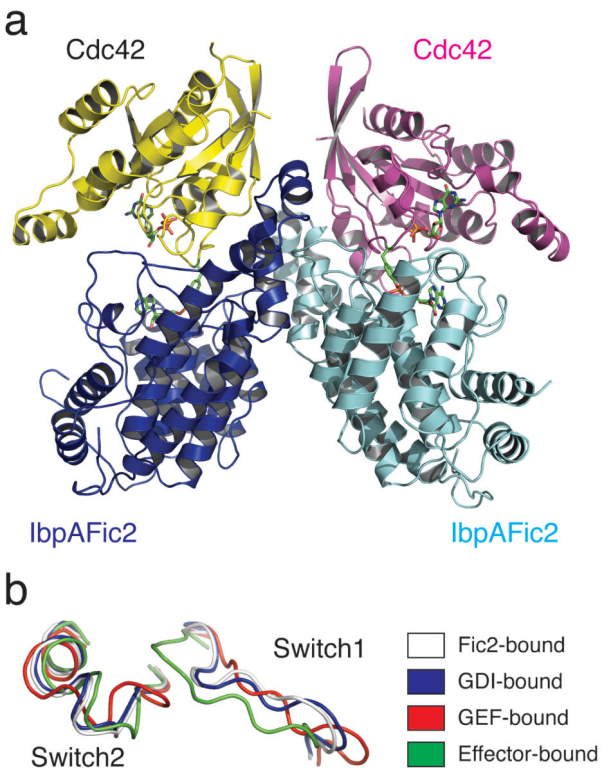

Figure 2.

Crystal structure of the IbpAFic2^{H3717A}-Cdc42 complex.

a. 2:2 IbpAFic2^{H3717A}: Cdc42 complex shown as ribbon diagrams. The two IbpAFic2^{H3717A} molecules are colored in blue and cyan, and the two Cdc42 molecules are colored in yellow and magenta, respectively. The bound GDP molecules and the adenylylated Tyr32 residues in the Cdc42 proteins are shown as sticks.

b. Cdc42 in the IbpAFic2^{H3717A}-Cdc42 complex adopts a conformation similar to the GDI-bound state. The Cdc42 molecule in the IbpAFic2^{H3717A}-Cdc42 complex is superposed with other Cdc42 structures, and their switch1 and switch2 regions are shown. White: Cdc42 in the IbpAFic2^{H3717A}-Cdc42 complex; blue: Cdc42 in the Cdc42-GDI complex (PDB ID: 1DOA24); red: Cdc42 in the Cdc42-GEF complex (PDB ID: 1KZ732); green: Cdc42 in the Cdc42-mDia1 (an effector protein of Cdc42) complex (PDB ID: 3EG533).

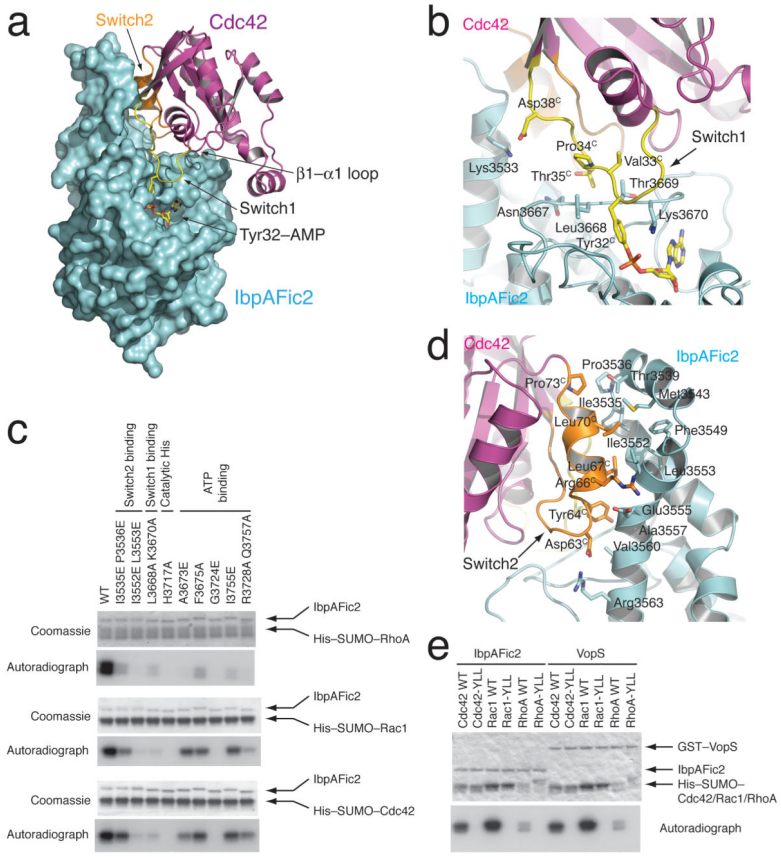

Figure 3.

IbpAFic2-Cdc42 binding interface.

a. An overall view of IbpAFic2-Cdc42 interface. IbpAFic2 is shown as a surface representation, and Cdc42 is shown as ribbon diagrams. The switch1 and switch2 regions of Cdc42 are highlighted in yellow and orange, respectively. The adenylylated Tyr32 residue in Cdc42 is shown as sticks.

b. A close view of the switch1 region interaction interface. IbpAFic2 and Cdc42 are shown as ribbon diagrams and colored in cyan and magenta, respectively. The switch1 region of Cdc42 is highlighted in yellow. The interacting residues from both molecules are labeled, and Cdc42 residues are denoted with superscript “C”.

c. IbpAFic2 mutants have impaired activities. IbpAFic2, wild-type or various mutants were incubated with recombinant RhoA, Rac1, and Cdc42 in the presence of α^{32}P-ATP as indicated. The reaction products were separated on SDS-PAGE and visualized by Commassie staining and autoradiography.

d. A close view of the switch2 region interaction interface. The switch2 region of Cdc42 is highlighted in orange.

e. IbpAFic2 and VopS cannot adenylylate switch2 mutants of RhoA, Rac1, and Cdc42. Cdc42-Y64A/L67E/L70E, Rac1-Y64A/L67E/L70E, and RhoAY66A/L69E/L72E were indicated as Cdc42-YLL, Rac1-YLL, and RhoA-YLL respectively for conciseness.

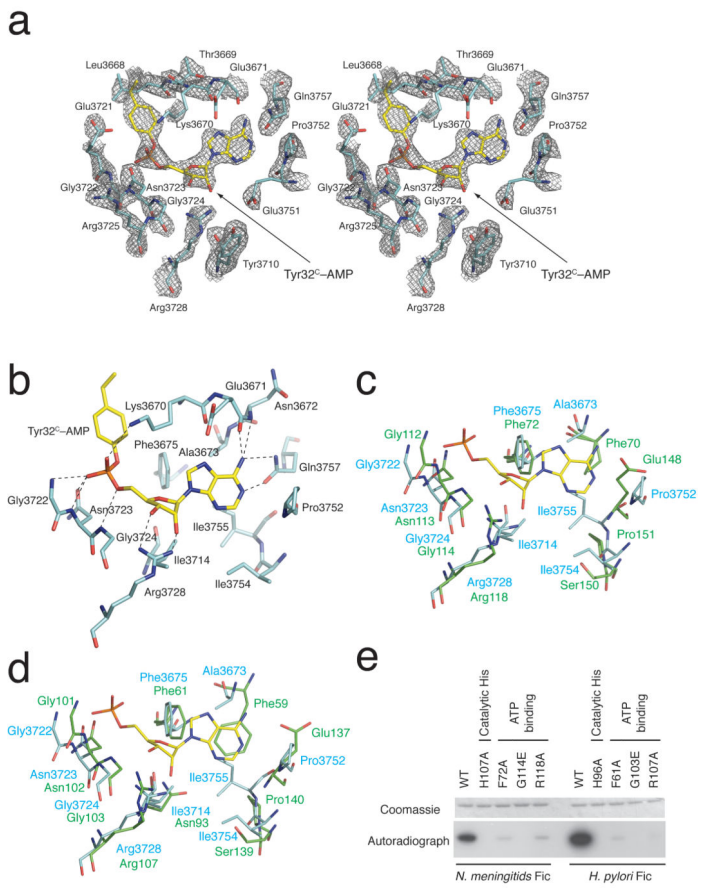

Figure 4.

Nucleotide binding by IbpAFic2.

a. Stereo view of a simulated annealing omit map (contoured at 1.1 σ) around the adenylylated tyrosine residue in the active site of IbpAFic2. The adenylylated tyrosine is omitted to calculate the map.

b. Interaction between IbpAFic2 and the AMP moiety of the adenylylated tyrosine. Hydrogen bond interactions are shown as dash lines.

c. The nucleotide-binding pocket of IbpAFic2 is superposed with *Neisseria meningitidis* Fic (PDB ID: 2G03). The carbon atoms of IbpAFic2 are colored in cyan, and the carbon atoms of N. meningitidis Fic are colored in green. The AMP moiety from the adenylylated tyrosine in the IbpAFic2^{H3717A}-Cdc42 complex structure is also shown. Residue Phe70 of *N. meningitidis* Fic is not displayed properly because of the existence of alternative conformation in the original PDB file.

d. The nucleotide-binding pocket of IbpAFic2 is superposed with *Helicobacter pylori* Fic (PDB ID: 2F6S). The carbon atoms of IbpAFic2 are colored in cyan, and the carbon atoms of *H. pylori* Fic are colored in green.

e. Mutation of residues corresponding to IbpAFic2 amino acids Phe3675, Gly3724, and Arg3728 in *N. meningitidis* Fic and *H. pylori* Fic reduced their auto-adenylylation.

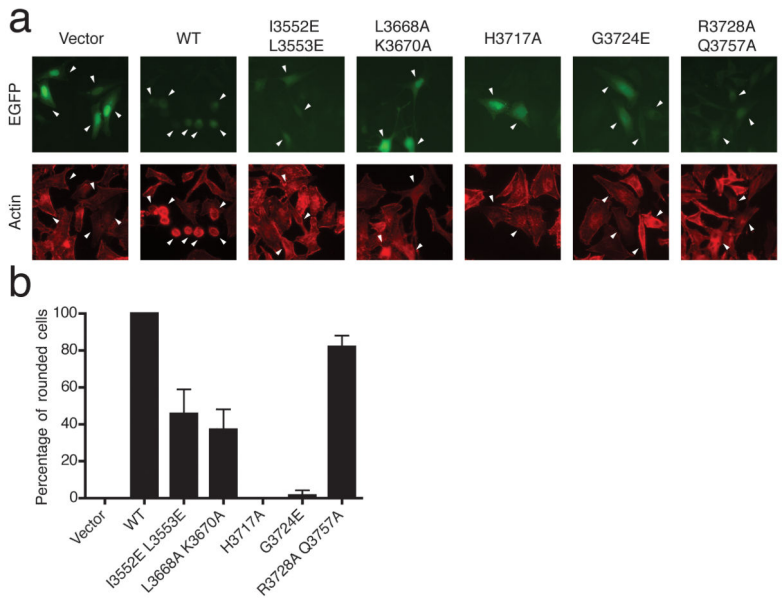

Figure 5.

IbpAFic2 mutants display reduced cytotoxicity.

a. EGFP-IbpAFic2, wild-type or various mutants were transfected into HeLa cells. Protein expression and cell morphology were visualized by EGFP fluorescence (top panels) and rhodamine phalloidin staining (bottom panels).

b. Percentage of transfected cells showing the rounding-up phenotype. Data represent the average of three independent experiments. Error bars represent the standard deviations.

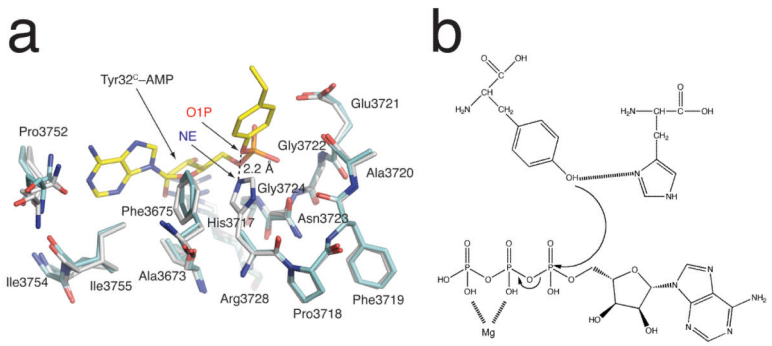

Figure 6.

A proposed catalytic mechanism of the Fic family proteins.

a. Structural superposition of wild-type IbpAFic2 and IbpAFic2^{H3717A} in the active site region. The carbon atoms of wild-type IbpAFic2 and IbpAFic2^{H3717A} are colored in white and cyan, respectively. The adenylylated tyrosine residue in the active site of IbpAFic2^{H3717A} is also shown.

b. A proposed catalytic mechanism of the Fic proteins.

Table 1

Data collection and refinement statistics

	IbpAFic2	IbpAFic2 Zn derivative	IbpAFic2^{H3717A}-Cdc42 Complex
Data collection			
Space group	$P3_121$	$P3_121$	$P2_12_12_1$
Cell dimensions			
a, *b*, *c* (Å)	64.38, 64.38, 149.69	64.25, 64.25, 149.20	63.50, 91.00, 190.97
α,β,γ (°)	90, 90, 120	90, 90, 120	90, 90, 90
Wavelength (Å)	1.0	1.2824	1.0
Resolution (Å)	1.85 (1.88–1.85)	2.0 (2.03–2.0)	2.3 (2.38–2.30)
R_{merge}	4.4 (60.6)	6.1 (35.5)	11.7 (44.7)
$I/\sigma I$	52.0 (3.0)	54.3 (6.7)	13.5 (2.0)
Completeness (%)	99.7 (98.5)	99.9 (100.0)	99.7 (97.3)
Redundancy	11.2 (9.0)	10.3 (10.6)	6.8 (4.0)
Refinement			
Resolution (Å)	1.85		2.3
No. reflections	31559		49831
R_{work}/R_{free}	21.2 / 24.2		18.2 / 23.2
No. atoms			
Protein	2293		7477
Ligand/ion	7		78
Water	204		792
B-factors			
Protein	51.3		27.3
Ligand/ion	46.8		26.9
Water	46.2		30.9
R.m.s. deviations			
Bond lengths (Å)	0.003		0.003
Bond angles (°)	0.682		0.793

*Each dataset was collected from a single crystal. *Values in parentheses are for highest-resolution shell.